This is a preprint manuscript. Please, download the final and much nicer version at:

https://doi.org/10.1021/acs.analchem.7b01734

Technical Note

Time-resolved luminescence spectroelectrochemistry at screen-printed electrodes. Following the redox-dependent fluorescence of [Ru(bpy)].

Daniel Martín-Yerga, Alejandro Pérez-Junquera, David Hernández-Santos, and Pablo Fanjul Bolado

Anal. Chem., **Just Accepted Manuscript** • DOI: 10.1021/acs.analchem.7b01734 • Publication Date (Web): 11 Sep 2017

Time-Resolved Luminescence Spectroelectrochemistry at Screen-Printed Electrodes. Following the Redox-Dependent Fluorescence of $[Ru(bpy)_3]^{2+}$.

Daniel Martín-Yerga, Alejandro Pérez-Junquera, David Hernández-Santos, Pablo Fanjul-Bolado*

DropSens, S.L., Ed. CEEI, Parque Tecnológico de Asturias, 33428 Llanera, Asturias, Spain

KEYWORDS: Spectroelectrochemistry, Screen-printed electrodes, Luminescence, Electrofluorescence, Electrochromism

ABSTRACT: In this work, a compact instrument for time-resolved luminescence spectroelectrochemistry using low-cost disposable electrodes is reported. This instrument can be coupled with screen-printed electrodes via a specific cell and a reflection probe, which allows to observe changes occurring at the electrode/solution interface. This approach allowed to follow the fluorescence variation of electrofluorochromic species such as $[Ru(bpy)_3]^{2+}$ at screen-printed carbon electrodes. A strong correlation between the electrochemical processes and the fluorescence was found during potentiostatic or multipulsed amperometric measurements. A decrease of the fluorescence was observed when the $[Ru(bpy)_3]^{2+}$ was oxidized to $[Ru(bpy)_3]^{3+}$ and part of this fluorescence is recovered when $[Ru(bpy)_3]^{3+}$ was reduced to the initial species. Moreover, a significant increment of the fluorescence was found when the oxygen reduction reaction takes place, which also confirms its quenching effect. Finally, multipulsed amperometric detection was employed in order to obtain more information about the redox-dependent luminescence of $[Ru(bpy)_3]^{2+}$ finding a continuous quenching over time attributed to bleaching chlorine-based species.

INTRODUCTION

Spectroelectrochemical techniques[1] combine simultaneous electrochemical and spectroscopic experiments, which allow to obtain optical information about different properties of electroactive species or electrochemical-based processes. The ideal feature of these techniques is the ability to get time-resolved in situ spectroscopic information from the electrochemical reactions. Different spectroscopic techniques have been coupled to electrochemical techniques, including molecular absorption (UV/VIS/IR)[2,3], luminescence[4,5], Raman[6] or electron spin resonance (ESR)[7]. Luminescence spectroelectrochemistry has been less explored than absorption spectroelectrochemistry due to the difficulty to design suitable cells to study the processes that occur at the electrode surface and the usual need to use the 90^0 or similar configurations between the excitation and emission lights[8]. These cells are not standardized and numerous works have focused on the development of proper spectroelectrochemical cells for their specific applications[9]. Most of these cells are fabricated as thin-layer systems, where the measured solution is confined in a small volume layer in contact with the working electrode. One of the first thin-layer cells for luminescence spectroelectrochemistry was reported by Yildiz et al.[10]. They studied the redox processes of rubrene, whose fluorescence depends on the oxidation state. Other authors have described similar thin-layer cell systems, but with other properties such as a long-optical path[11,12], with variable thickness of the thin-layer[4,13], for nonaqueous solvents[14] for oxygen-free measurements[15] or for coupling benchtop spectrophotometers[16]. Different kinds of electrodes have been coupled in these thin-layer cells such as deposited metallic films[10], transparent conducting oxide films[16] or minigrid electrodes[17,18]. In other cases, the fluorescence of films adsorbed on electrodes has been studied, where the cell properties (volume, configuration, path) does not have as much impact on the optical detection because the species are confined on the electrode surface[19,20]. Fluorescence spectroelectrochemistry has also been widely used for imaging applications with spatial resolution after coupling with microscopy systems[21]. For instance, it has been used for single particle tracking analysis to study the redox properties of Nile Red confined in emulsion droplets[22], for imaging fluxes of redox reactions[23,24], to study and imaging DNA self-assembled monolayers at gold electrodes[25], to localize and size electroactive defects of insulating layers[26] or to follow corrosion processes[27,28]. All these instrumental systems have proven useful for specific applications and may have interesting properties such as a short time to produce total electrolysis (thin-layer cells) compared to other setups[29] or spatial resolution, but they also have some drawbacks such as the difficult cell fabrication and assembly or the cleaning steps between assays, which can influence the precision between experiments, or the complex and costly instrumentation needed (for fluorescence-enabled electrochemical microscopy). The spectroelectrochemical cells are also specifically designed for certain electrodes and, therefore, they are not compatible with other electrodes such as the widely employed, screen-printed electrodes. A simpler approach was described by Schroll et al. where they performed luminescence spectroelectrochemistry in a micro-drop using a reflection probe in a near-normal position to the electrode surface (epifluorescence mode), aplying the setup to semi-infinite diffusion studies in a bulk solution[30] or by forcing the thin-layer, working in complete electrolysis conditions, by moving the probe towards the micro-drop in contact with the electrode[31], which demonstrates the utility of this setup.

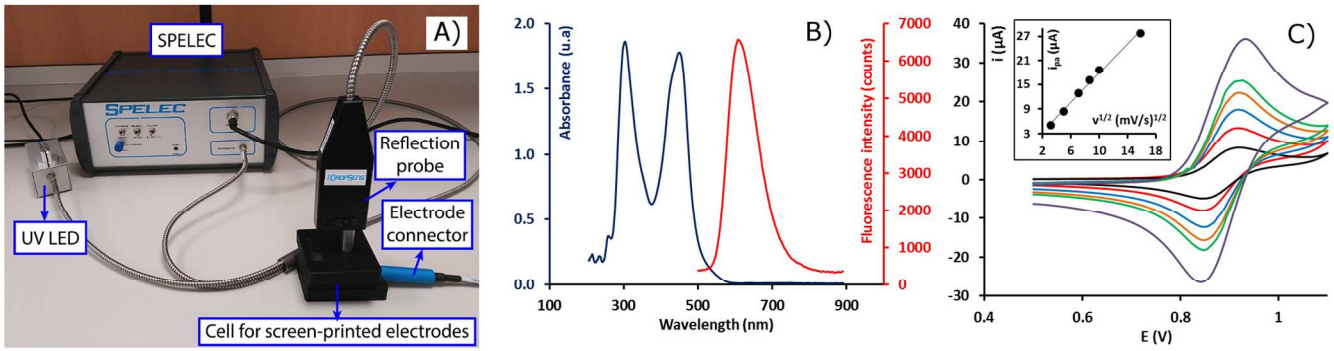

Figure 1. A) Image of the instrumentation employed for luminescence spectroelectrochemistry at screen-printed electrodes. B) UV/VIS absorption (blue line) and fluorescence (red line) spectra of $[Ru(bpy)_3]^{2+}$ in 0.1 M KNO_3. C) Voltammograms of 1.5 mM $[Ru(bpy)_3]^{2+}$ in 0.1 M KNO_3 at several scan rates (10-250 mV/s) by applying a potential sweep between +0.5 V and +1.1 V. Inset shows the dependence of the anodic peak current (i_{pa}) with the square root of the scan rate.

In epifluorescence mode[32], also called specular reflection, the light is passed through the sample, reflected off the electrode surface and then passed back through the sample. Most luminescent species, because their chemical structure, are usually species that adsorb extremely well on different surfaces, so it is necessary to clean the electrodes after performing the measurements, leading to more complex procedures and a possible reduction of the precision between assays. For these reasons, the development of compact luminescence spectroelectrochemical systems that could be easily used with low-cost disposable electrodes could be quite useful for the study of the fluorescent properties of electroactive species.

The luminescence of certain elecrofluorochromic species[33,34] can be switched via electrically driven redox reactions so they have applications in different fields like sensing[35] or optical devices[36,37].Speectroelectrochemical techniques are the most suitable to characterize the mechanisms involved in electrofluorochromic species as they can record simultaneously the electrochemical and optical responses. For instance, the reduction of ethidium bromide38, redox processes of riboflavin39 and bilirubin40 or different kinds of fluorescent films[19,20] or other electrofluorochromic species[41,42] have been studied. $[Ru(bpy)_3]^{2+}$ is one of the electrofluorochromic model species usually studied since its fluorescence changes according to its oxidation state[43]. For example, the fluorescence quenching of $[Ru(bpy)_3]^{2+}$ by quinones at different applied potentials[44], their luminescent behaviour at a liquid/liquid interface of water/1,2-dichloroethane[45] or in polymeric films[43,46], in ordered nanoporous systems[47] or the monitorization of concentration gradients in real-time[48] was studied. However, as far as we know, spectroelectrochemical studies of electroluminochromic species at screen-printed electrodes have not been described so far.

In this work, we report a compact and simple equipment for time-resolved in situ luminescence spectroelectrochemistry. This instrument allows to record complete emission spectra continuously (high time-resolution) and simultaneously (totally synchronized) during the electrochemical measurement. It can be coupled to a reflection probe (epifluorescence mode) placed on a simple spectroelectrochemical cell for assays using miniaturized disposable screen-printed electrodes. This setup allows the utilization of disposable electrodes with a high precision between assays because both the probe and the electrodes are placed easily in the same position. After the measurement, the cell can be opened, another disposable electrode can be placed again and a new spectroelectrochemical experiment can be performed quickly, avoiding tedious cleaning of the electrode surface or the cell compartiment. The ease of performing luminescence spectroelectrochemistry with this compact and integrated setup is demonstrated studying the redox-dependent fluorescence of $[Ru(bpy)_3]^{2+}$ finding a strong correlation with the electrochemical processes that take place at the surface of screen-printed electrodes.

MATERIALS AND METHODS

Instrumentation

All electrochemical, spectroscopic and spectroelectrochemical measurements were carried out with a SPELEC instrument (DropSens) controlled by DropView SPELEC software. Fluorescence and luminescence spectroelectrochemistry measurements were performed with a bifurcated reflection probe (DropSens, DRP-FLUOPROBE) and a specific cell for screen-printed electrodes (Dropsens, DRP-RAMANCELL) working in a near-normal reflection configuration. The excitation connector of the bifurcated probe was connected to a 395 nm UV LED (DRP-UVLED, DropSens) and the detection connector of the probe was connected to the SPELEC. The LED was powered by an USB port of the computer and its intensity was changed with the selector on the LED box (3.5 V was the applied voltage in this work). UV/VIS absorption measurements were performed using a cuvette holder (CUV-ALL-UV, Ocean Optics) for 1 cm pathlength cuvettes and a 10 ms integration time. Figure 1A shows the SPELEC setup for time-resolved luminescence spectroelectrochemistry with screen-printed electrodes. Fluorescence measurements were carried out with an integration time of 250 ms, recording each full spectrum in this time (from 200 to 900 nm). The normalized fluorescence was calculated as the ratio between the fluorescence intensity and the initial fluorescence intensity before the spectroelectrochemical experiment.

DropSens screen printed carbon electrodes (SPCEs, DRP-110) incorporate a three-electrode configuration printed on a planar ceramic substrate (with dimensions of 3.4 x 1.0 cm). Both working (disk-shaped 4 mm diameter) and counter electrodes are made of carbon inks, whereas pseudoreference electrode and electric contacts are made of silver. Therefore, the potential values are reported versus the silver pseudoreference elec-

trode. These electrodes have been previously characterized by microscopic and electrochemical techniques in numerous works[49–52]. Silver ions in solution could act as fluorescence quenchers, however 0.1 M KNO_3 electrolyte solution is used in this work, so no silver ions are expected to be released to the solution due to an oxidation process from the reference electrode and no experimental evidence about this effect was observed. All measurements with SPCEs were carried out at room temperature and using an aliquot of 45 µL of the appropriate solution. SPCEs were connected to the SPELEC instrument through a specific connector (DropSens, DRP-CAST).

Reagents and solutions

Tris(2,2'-bipyridyl)dichlororuthenium(II) hexahydrate ($[Ru(bpy)_3]^{2+}$), potassium chloride and potassium nitrate were purchased from Sigma-Aldrich. Ultrapure water was obtained from a Milli-RO 3 plus/Milli-Q plus 185 purification system from Millipore.

Digital simulations

Digital simulations of cyclic voltammetry were performed using a Python software (simEC) developed by D. Martín-Yerga based on the work proposed by Brown[53].

RESULTS AND DISCUSSION

Spectroscopic and electrochemical characterization of $[Ru(bpy)_3]^{2+}$

The spectroscopic characterization of $[Ru(bpy)_3]^{2+}$ was carried out by UV/VIS absorption and fluorescence spectroscopy. The absorption spectrum of 0.5 mM $[Ru(bpy)_3]^{2+}$ in 0.1 M KNO3 (Figure 1B) shows a good absorption range between 240-550 nm with two peak maxima near 300 and 450 nm, which could be tentatively assigned to π-π^* and metal-to-ligand charge transfers, respectively[54]. In order to use the spectroelectrochemical system in reflection mode, an UV LED with a maximum emission at 395 nm was chosen because it allowed detecting the fluorescence of $[Ru(bpy)_3]^{2+}$ without interference of the excitation light. Thus, although the wavelength of this LED does not correspond exactly to the maximum absorption band of the $[Ru(bpy)_3]^{2+}$, the excitation with this light was enough to produce a significant fluorescence. Figure 1B also shows the emission spectrum of 1.5 mM $[Ru(bpy)_3]^{2+}$ with an intense band at 610 nm using the reflection probe and screen-printed carbon electrodes, which demonstrates that this configuration is suitable for detection of fluorescent species.

The electrochemical processes of $[Ru(bpy)_3]^{2+}$ at SPCEs in 0.1 M KNO_3 were studied. Figure 1C shows the cyclic voltammograms obtained in the potential range between +0.5 V and +1.1 V at several scan rates. A reversible redox process corresponding to the oxidation of $[Ru(bpy)_3]^{2+}$ to $[Ru(bpy)_3]^{3+}$ and its corresponding reduction is observed. The peak potential of the oxidation process was +0.913 V and for the reduction process was +0.852 V, with a peak potential difference around 61 mV for all scan rates. This fact indicates that these processes are fast, reversible and with a good Nernstian behaviour. Both the anodic and cathodic peak currents increased linearly with the square root of the scan rate (see inset of the Figure 1C for the anodic peak current), indicating a diffusion-controlled electrochemical reaction. This has been confirmed by digital simulation of electrochemical reactions controlled by semi-infinite diffusion (see Supporting Information, Figure S1), which is well correlated with the experimental behavior obtained at different scan rates A heterogeneous rate constant of $5x10^{-2}$ cm/s was estimated, indicating the fast electron transfer. The reversible behaviour of these species is especially interesting for spectroelectrochemical studies since the $[Ru(bpy)_3]^{2+}$ is fluorescent but $[Ru(bpy)_3]^{3+}$ is non-fluorescent.

Time-resolved luminescence spectroelectrochemical studies of $[Ru(bpy)_3]^{2+}$

A time-resolved spectroelectrochemical study using cyclic voltammetry for the electrochemical activation was performed in order to visualize the fluorescence response of the electrofluorochromic species at screen-printed carbon electrodes as the potential changes over time. A solution of 1.5 mM $[Ru(bpy)_3]^{2+}$ in 0.1 M KNO_3 was used for the following experiments. The potential was applied from 0 V to +1.2 V to -1.2 V with the final potential again being 0 V at a scan rate of 10 mV/s. Under these conditions one full spectrum was recorded every 2.5 mV (250 ms as integration time). A low background fluorescent signal was obtained in absence of $[Rubpy)_3]^{2+}$ as shown in Figure S2, suggesting a low influence of the screen-printed electrode and the cell materials on the recorded signal. The intensity of the fluorescence band at 610 nm showed a strong correlation with the different electrochemical processes observed at the electrode/solution interface as can be seen dynamically in the Video S1 (S. I.). To follow the changes in the fluorescence, the voltafluorogram and the derivative voltafluorogram representations were very useful. Figure 2A shows the fluorescence variation at 610 nm relative to the applied potential (voltafluorogram) and Figure 2B displays the derivative of the fluorescence variation with the potential (derivative voltafluorogram), which provides information on slope changes in the voltafluorogram. Initially, the fluorescence is kept relatively constant from 0 V to +0.80 V. At a potential near +0.80 V, there is a slope change that results in a pronounced decrease in fluorescence leading to a peak response in the derivative curve. This change shows a high correlation with the anodic oxidation process of $[Ru(bpy)_3]^{2+}$ to $[Ru(bpy)_3]^{3+}$, with the peak potential in the derivative curve (+0.912 V) similar to the peak potential of the voltammogram (+0.913 V). The fluorescence decreased until a potential near +0.90 V of the reverse sweep, in which a cathodic process corresponding to the reduction of $[Ru(bpy)_3]^{3+}$ to $[Ru(bpy)_3]^{2+}$ appeared, where the fluorescence intensity begins to grow again. This change in the trend led to a new increasing peak in the derivative voltafluorogram (+0.846 V) with a peak potential close to the voltammetric peak potential (6 mV difference). The peak potential difference for the $[Ru(bpy)_3]^{2+/3+}$ redox couple in the derivative voltafluorogram was 66 mV, similar to that obtained in the voltammetric measurements (61 mV).

This behavior is the expected one as reported in the literature because the $[Ru(bpy)_3]^{3+}$ is a non-fluorescent species. However, as can be seen in Figure 2A, the fluorescence intensity does not reach the level observed initially, so it seems that some of the fluorescence of the initial species has been irreversibly lost (see below for more insight into this fact). At a potential near -0.60 V, there is a new trend change in the fluorescence, with a significant increment towards more negative potentials, which correlates with a new cathodic process that appeared in the voltammogram.

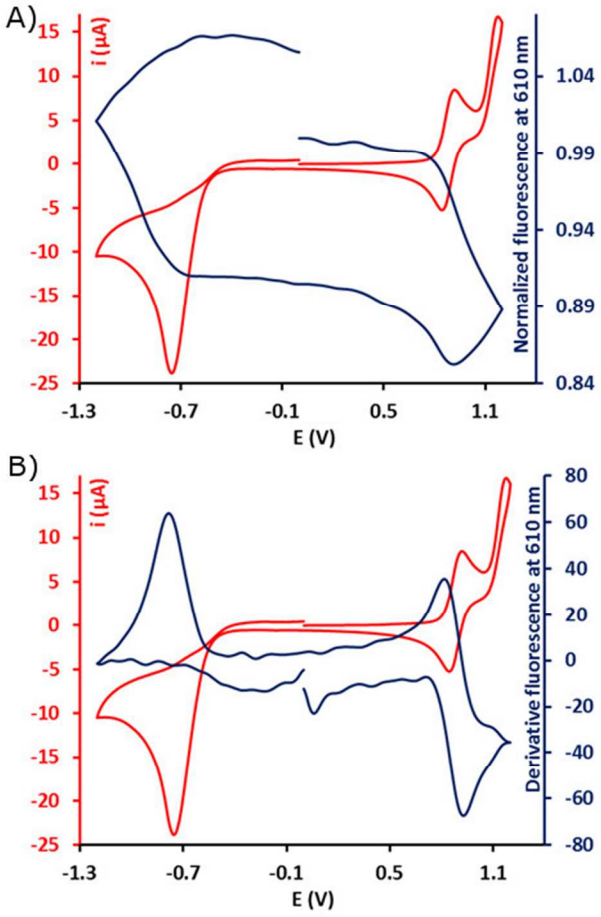

Figure 2. A) Voltafluorogram of the normalized fluorescence at 610 nm (blue line) during the cyclic voltammogram (red line) of 1.5 mM $[Ru(bpy)_3]^{2+}$ in 0.1 M KNO_3 at 10 mV/s. B) Derivative voltafluorogram at 610 nm (blue line) during the cyclic voltammogram (red line) of 1.5 mM $[Ru(bpy)_3]^{2+}$ in 0.1 M KNO_3 at 10 mV/s.

This process is attributed to the oxygen reduction reaction (ORR)[55], as it was confirmed by performing measurements of the analyte and the electrolyte solution (0.1 KNO_3) in normal and deareated solutions (Figure S3). Oxygen acts as a fluorescent quencher usually by dynamic collisions between molecules producing energy-transfer processes[56], and therefore, their presence in the solution leads to a basal quenching of the fluorescence of $[Ru(bpy)_3]^{2+}$ as has been previously reported in the literature[57,58]. More specifically, the dynamic quenching mechanism seems to come from collisions between excited-state fluorophores with triplet-state O_2 molecules to produce the ground-state fluorophore and a low-energy singlet O_2[56,57]. The reduction of the oxygen at the electrode surface allows to decrease the local concentration of oxygen and the probability of collisions with the molecules of $[Ru(bpy)_3]^{2+}$. The correlation between the fluorescence-ORR can be observed in the derivative voltafluorogram with a peak similar to the ORR voltammetric peak. A new decrease of the fluorescence is found at the last range of the potential sweep (from -0.5 to 0 V), which can be attributed to the diffusion of new oxygen molecules acting again as quenchers from the solution to the electrode interface, and showing that the luminescent spectroelectrochemistry with this setup could also provide information about non-redox processes. Therefore, these studies show that the $[Ru(bpy)_3]^{2+}$ fluorescence correlates well with the redox processes found at screen-printed carbon electrodes. In addition, the derivative of the fluorescence resembles the voltammogram but inversely: the anodic processes cause a decrease in the fluorescence at 610 nm, while that the cathodic processes cause an increase in the fluorescence.

In order to further study the electrofluorochromic response of $[Ru(bpy)_3]^{2+}$ at screen-printed electrodes, several cycles of discrete potential controlled pulses of +1.2 V (60 s) and +0.3 V (60 s) were consecutively applied. The response can be observed dynamically in the Video S2 (S.I.). These pulses are able to produce the oxidation and the reduction of the $[Ru(bpy)_3]^{2+/3+}$ in a cyclic way. Figure 3A shows the variation of the fluorescence at 610 nm over time. The fluorescence decreased with the pulses at +1.2 V since it causes the oxidation of $[Ru(bpy)_3]^{2+}$ to non-fluorescent $[Ru(bpy)_3]^{3+}$, and the pulses at +0.3 V led to an increase of the fluorescence by the regeneration of the fluorescent $[Ru(bpy)_3]^{2+}$. The derivative voltafluorogram (Figure 3B) shows a high correlation with the recorded electrochemical response. However, the fluorescence does not recover completely to the initial values and a continuous decreasing trend is observed for the first cycles. Starting from a specific time, the fluorescence is kept at constant values with the on/off pulses of the redox processes. This fact suggests that some irreversible quenching of the fluorescence of $[Ru(bpy)_3]^{2+}$ happened only during the first cycles of this experiment, and then the origin of this quenching ceased. The $[Ru(bpy)_3]^{2+/3+}$ redox couple shows a good and reversible electrochemical behavior, which suggests that all the electrogenerated $[Ru(bpy)_3]^{3+}$ can be reduced to the initial form. Then, the irreversible quenching should come from external species in the solution, which are consumed during the first pulses. As the $[Ru(bpy)_3]^{2+}$ salt is chloride-based, the influence of chloride ion on the electrofluorochromic response of $[Ru(bpy)_3]^{2+}$ was evaluated. The same experiment but with a 0.1 M KCl electrolyte solution was performed. The variation of the fluorescence in relation to the electrochemical response is shown in the Figure 3C. In this case, a faster decrease of the fluorescence with the different pulse cycles was observed until the complete quenching of the fluorescence, which then could not be recovered. This suggests that chloride ion has a negative effect on the $[Ru(bpy)_3]^{2+}$ fluorescence. However, this fluorescence behavior is not observed in a solution at open circuit potential, so it should originate from a potential-dependent reaction. Chloride could be oxidized at positive potentials (near the oxidation of $[Ru(bpy)_3]^{2+}$), and the electrogenerated chlorine-based species could act as fluorescence quenchers. This effect is much faster and more determinant at a higher chloride concentration (0.1 M from the electrolyte vs. 3 mM from $[Ru(bpy)_3]^{2+}$ salt) as shown in Figure 3C, even removing completely the fluorescence of $[Ru(bpy)_3]^{2+}$.

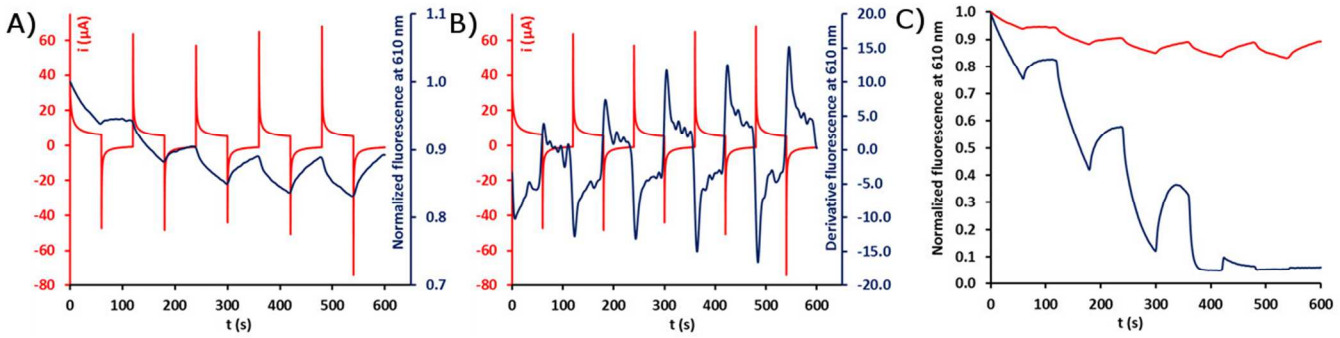

Figure 3. A) Time-resolved evolution of the normalized fluorescence at 610 nm (blue line) during the multipulsed amperometry (red line) of 1.5 mM $[Ru(bpy)_3]^{2+}$ in 0.1 M KNO_3. Multipulsed amperometry was performed by applying 5 cycles of +1.2 V and +0.3 V for 60 s. B) Evolution of the derivative fluorescence at 610 nm (blue line) over time for the previously described multipulsed amperometry experiment (red line). C) Time-resolved evolution of the normalized fluorescence at 610 nm during the multipulsed amperometry of 1.5 mM $[Ru(bpy)_3]^{2+}$ in 0.1 M KNO_3 (red line) and in 0.1 M KCl (blue line).

CONCLUSIONS

In this work, a simple and compact instrument for luminescence spectroelectrochemistry using low-cost disposable screen-printed electrodes is reported. This system allowed to observe easily and in real time, the changes of $[Ru(bpy)_3]^{2+}$ fluorescence when different electrochemical processes take place at screen-printed electrode surfaces. These studies have shown that the fluorescence of $[Ru(bpy)_3]^{2+}$ can be modulated according to the applied potential at screen-printed electrodes, which leads to the oxidation of $[Ru(bpy)_3]^{2+}$ to $[Ru(bpy)_3]^{3+}$, with different luminescent properties. However, the initial fluorescence is not totally recovered after the reduction to the initial species, and a decrease over time was observed by applying several cycles of modulation. We propose that chloride oxidation could be responsible for the quenching by generation of bleaching chlorine-based species at the electrode surface. Moreover, an increment in the fluorescence has also been observed when the oxygen is reduced, which confirms its quenching effect in real time, and therefore, it is other important parameter for modulating $[Ru(bpy)_3]^{2+}$ electrofluorescence in aqueous solutions.

ASSOCIATED CONTENT

Supporting Information

The Supporting Information is available free of charge on the ACS Publications website. Digital simulation results. Background fluorescence spectrum. Voltammograms in deareated solution. Video S1 shows the normalized fluorescence and the derivative during the potentiodynamic experiment. Video S2 shows the normalized fluorescence and the derivative during the multipulsed experiment. Video S3 shows the results of the digital simulation results in a dynamic and visual way.

AUTHOR INFORMATION

Corresponding Author

*E-mail: pfanjul@dropsens.com

Author Contributions

All authors have given approval to the final version of the manuscript.

REFERENCES

(1) Kaim, W.; Fiedler, J. *Chem. Soc. Rev.* **2009**, *38*, 3373–3382.

(2) González-Diéguez, N.; Colina, A.; López-Palacios, J.; Heras, A. *Anal. Chem.* **2012**, *84*, 9146–9153.

(3) Hernández, C. N.; García, M. B. G.; Santos, D. H.; Heras, M. A.; Colina, A.; Fanjul-Bolado, P. *Electrochem. commun.* **2016**, *64*, 65–68.

(4) Dias, M.; Hudhomme, P.; Levillain, E.; Perrin, L.; Sahin, Y.; Sauvage, F.-X.; Wartelle, C. *Electrochem. commun.* **2004**, *6*, 325–330.

(5) Barrera, J.; Ibañez, D.; Heras, A.; Ruiz, V.; Colina, A. *J. Phys. Chem. Lett.* **2017**, *8*, 531–537.

(6) Ibañez, D.; Garoz-Ruiz, J.; Heras, A.; Colina, A. *Anal. Chem.* **2016**, *88*, 8210–8217.

(7) Petr, A.; Dunsch, L.; Neudeck, A. *J. Electroanal. Chem.* **1996**, *412*, 153–158.

(8) Kirchhoff, J. *Curr. Sep.* **1997**, *16*, 11–14.

(9) Timm, R. A.; da Silva, E. T. S. G.; Bassetto, V. C.; Abruña, H. D.; Kubota, L. T. *Electrochim. Acta* **2017**, *232*, 150–155.

(10) Yildiz, A.; Kissinger, P. T.; Reilley, C. N. *Anal. Chem.* **1968**, *40*, 1018–1024.

(11) Simone, M. J.; Heineman, W. R.; Kreishman, G. P. *Anal. Chem.* **1982**, *54*, 2382–2384.

(12) Lee, Y. F.; Kirchhoff, J. R. *Anal. Chem.* **1993**, *65*, 3430–3434.

(13) Yu, J.-S.; Yang, C.; Fang, H.-Q. *Anal. Chim. Acta* **2000**, *420*, 45–55.

(14) Rhodes, R. K.; Kadish, K. M. *Anal. Chem.* **1981**, *53*, 1539–1541.

(15) Compton, R. G.; Fisher, A. C.; Wellington, R. G. *Electroanalysis* **1991**, *3*, 27–29.

(16) Wilson, R. A.; Pinyayev, T. S.; Membreno, N.; Heineman, W. R. *Electroanalysis* **2010**, *22*, 2162–2166.

(17) Heineman, W. R.; Norris, B. J.; Goelz, J. F. *Anal. Chem.* **1975**, *47*, 79–84.

(18) Jones, E. T. T.; Faulkner, L. R. *J. Electroanal. Chem. Interfacial Electrochem.* **1984**, *179*, 53–64.

(19) Jennings, P.; Jones, A. C.; Mount, A. R. *Phys. Chem. Chem. Phys.* **2000**, *2*, 1241–1248.

(20) Jin, L.; Shang, L.; Zhai, J.; Li, J.; Dong, S. *J. Phys. Chem. C* **2010**, *114*, 803–807.

(21) Bouffier, L.; Doneux, T. *Curr. Opin. Electrochem.* **2017**, in press.

(22) Batchelor-McAuley, C.; Little, C. A.; Sokolov, S. V.; Kätelhön, E.; Zampardi, G.; Compton, R. G. *Anal. Chem.* **2016**, *88*, 11213–11221.

(23) Yang, M.; Batchelor-McAuley, C.; Kätelhön, E.; Compton, R. G. *Anal. Chem.* **2017**, *89*, 6870–6877.

(24) Oja, S. M.; Zhang, B. *Anal. Chem.* **2014**, *86* , 12299–12307.

(25) Meunier, A.; Triffaux, E.; Bizzotto, D.; Buess-Herman, C.; Doneux, T. *ChemElectroChem* **2015**, *2*, 434–442.

(26) Renault, C.; Marchuk, K.; Ahn, H. S.; Titus, E. J.; Kim, J.; Willets, K. A.; Bard, A. J. *Anal. Chem.* **2015**, *87*, 5730–5737.

(27) Liu, X.; Spikes, H.; Wong, J. S. S. *Corros. Sci.* **2014**, *87*, 118–126.

(28) Panova, A. A.; Pantano, P.; Walt, D. R. *Anal. Chem.* **1997**, *69*, 1635–1641.

(29) Tan, L.; Xie, Q.; Yao, S. *Electroanalysis* **2004**, *16*, 1592–1597.

(30) Schroll, C. A.; Chatterjee, S.; Heineman, W. R.; Bryan, S. A. *Anal. Chem.* **2011**, *83*, 4214–4219.

(31) Schroll, C. A.; Chatterjee, S.; Heineman, W. R.; Bryan, S. A. *Electroanalysis* **2012**, *24*, 1065–1070.

(32) Miomandre, F.; Audebert, P. *Luminescence in Electrochemistry*; Miomandre, F., Audebert, P., Eds.; Springer International Publishing: Cham, 2017.

(33) Sun, J.; Chen, Y.; Liang, Z. *Adv. Funct. Mater.* **2016**, *26*, 2783–2799.

(34) Al-Kutubi, H.; Zafarani, H. R.; Rassaei, L.; Mathwig, K. *Eur. Polym. J.* **2016**, *83*, 478–498.

(35) Ding, G.; Zhou, H.; Xu, J.; Lu, X. *Chem. Commun.* **2014**, *50*, 655–657.

(36) Kuo, C.-P.; Chang, C.-L.; Hu, C.-W.; Chuang, C.-N.; Ho, K.-C.; Leung, M. *ACS Appl. Mater. Interfaces* **2014**, *6*, 17402–17409.

(37) Neo, W. T.; Ye, Q.; Chua, S.-J.; Xu, J. *J. Mater. Chem. C* **2016**, *4*, 7364–7376.

(38) Hu, X.; Wang, Q.; He, P.; Fang, Y. *Anal. Sci.* **2002**, *18*, 645–650.

(39) Chen, W.; Chen, J. J.; Lu, R.; Qian, C.; Li, W. W.; Yu, H. Q. *Bioelectrochemistry* **2014**, *98*, 103–108.

(40) Niu, J.; Dong, S. *Electroanalysis* **1995**, *7*, 1059–1062.

(41) Kim, Y.; Do, J.; Kim, E.; Clavier, G.; Galmiche, L.; Audebert, P. *J. Electroanal. Chem.* **2009**, *632*, 201–205.

(42) Miomandre, F.; Stancheva, S.; Audibert, J.-F.; Brosseau, A.; Pansu, R. B.; Lepeltier, M.; Mayer, C. R. *J. Phys. Chem. C* **2013**, *117*, 12806–12814.

(43) Moretto, L. M.; Kohls, T.; Chovin, A.; Sojic, N.; Ugo, P. *Langmuir* **2008**, *24*, 6367–6374.

(44) Goulle, V.; Harriman, A.; Lehn, J.-M. *J. Chem. Soc. Chem. Commun.* **1993**, *27*, 1034–1036.

(45) Ding, Z.; Wellington, R. G.; Brevet, P. F.; Girault, H. H. *J. Phys. Chem.* **1996**, *100*, 10658–10663.

(46) Kaval, N.; Seliskar, C. J.; Heineman, W. R. *Anal. Chem.* **2003**, *75*, 6334–6340.

(47) Chovin, A.; Garrigue, P.; Servant, L.; Sojic, N. *ChemPhysChem* **2004**, *5*, 1125–1132.

(48) Amatore, C.; Chovin, A.; Garrigue, P.; Servant, L.; Sojic, N.; Szunerits, S.; Thouin, L. *Anal. Chem.* **2004**, *76*, 7202–7210.

(49) Fanjul-Bolado, P.; Hernández-Santos, D.; Lamas-Ardisana, P. J.; Martín-Pernía, A.; Costa-García, A. *Electrochim. Acta* **2008**, *53*, 3635–3642.

(50) Kadara, R. O.; Jenkinson, N.; Banks, C. E. *Sensors Actuators B Chem.* **2009**, *138*, 556–562.

(51) Martín-Yerga, D.; Costa Rama, E.; Costa García, A. *J. Chem. Educ.* **2016**, *93*, 1270–1276.

(52) Mistry, K. K.; Sagarika Deepthy, T.; Chau, C. R.; Saha, H. *Curr. Sci.* **2015**, *109*, 1427.

(53) Brown, J. H. *J. Chem. Educ.* **2015**, *92*, 1490–1496.

(54) Thompson, D. W.; Ito, A.; Meyer, T. J. *Pure Appl. Chem.* **2013**, *85*, 1257–1305.

(55) Martín-Yerga, D.; Costa-García, A. *Phys. Chem. Chem. Phys.* **2017**, *19*, 5018–5027.

(56) Schweitzer, C.; Schmidt, R. *Chem. Rev.* **2003**, *103*, 1685–1758.

(57) Rusak, D. A.; James, W. H.; Ferzola, M. J.; Stefanski, M. J. *J. Chem. Educ.* **2006**, *83*, 1857.

(58) Morris, K. J.; Roach, M. S.; Xu, W.; Demas, J. N.; DeGraff, B. A. *Anal. Chem.* **2007**, *79*, 9310–9314.

Table of Contents artwork

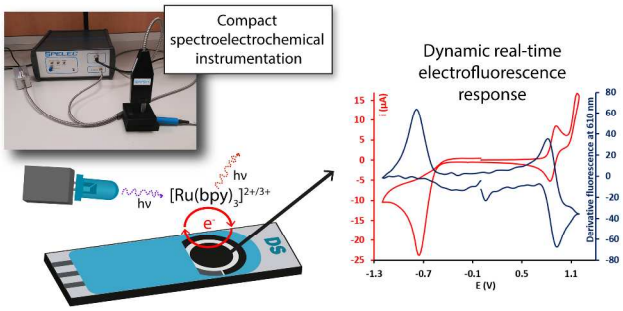

LUMINESCENCE SPECTROELECTROCHEMISTRY AT SCREEN-PRINTED ELECTRODES

SUPPORTING INFORMATION

Time-Resolved Luminescence Spectroelectrochemistry at Screen-Printed Electrodes. Following the Redox-Dependent Fluorescence of $[Ru(bpy)_3]^{2+}$.

Daniel Martín-Yerga, Alejandro Pérez-Junquera, David Hernández-Santos, Pablo Fanjul-Bolado*

[1]*DropSens S.L. Edificio CEEI, Parque Tecnológico de Asturias, 33428 Llanera, Asturias, Spain*

* Corresponding author: pfanjul@dropsens.com

DIGITAL SIMULATION STUDY

Digital simulation of the cyclic voltammetry of $[Ru(bpy)_3]^{2+/3+}$ was performed by using a Python software (simEC) developed by D. Martín-Yerga and based on the work by Brown[1], which makes the calculations by following Butler-Volmer kinetics. Some parameters for the digital simulation were: temperature (293.15 K), gas constant (8.31451 J/mol K), Faraday constant (96485 C/mol). Electrode area was 0.08 cm^2 as it was previously experimentally calculated for screen-printed carbon electrodes[2], and the diffusion coefficient for $[Ru(bpy)_3]^{2+/3+}$ was estimated by voltammetric measurements ($5x10^{-6}$ cm^2/s) and a similar value was assumed for the oxidized and reduced species. **Figure S1** shows the digital simulation results in a graphical way and **Video S3** shows these results dynamically together with the evolution of the profile concentration of $[Ru(bpy)_3]^{2+}$ (red line) and $[Ru(bpy)_3]^{3+}$ (blue line). This demonstrates how the concentration of the species and the diffusion layer changed with the potential during the simulated cyclic voltammetry. As observed in the figures, the experimental results are well correlated with the simulation results obtaining a good fitting with a heterogeneous rate constant of $5x10^{-2}$ cm/s, a value typically considered as a reversible electron transfer. Therefore, these studies suggest that the electrochemical reaction of the $[Ru(bpy)_3]^{2+/3+}$ redox couple is fast(reversible) and it is controlled by the semi-infinite linear diffusion.

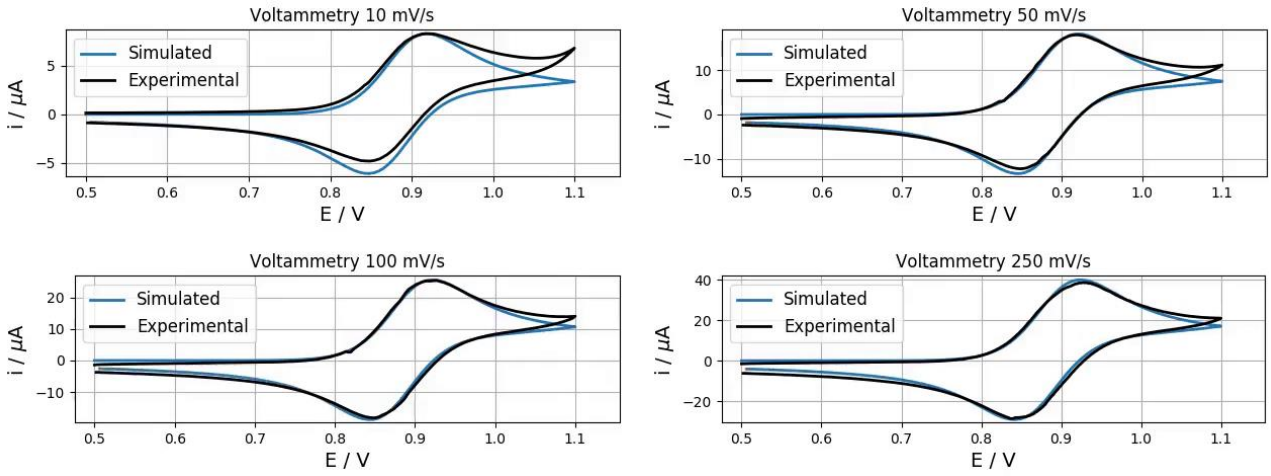

Figure S1. Results of the digital simulation of the cyclic voltammetry of $[Ru(bpy)_3]^{2+/3+}$ compared to the experimental results obtained at different scan rates (10, 50, 100 and 250 mV/s).

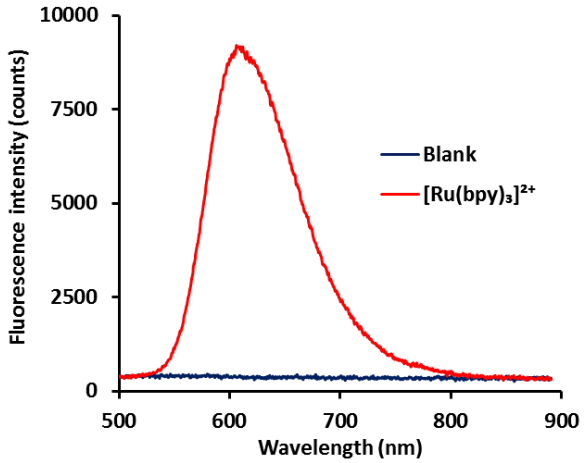

Figure S2. Fluorescence spectra for a blank solution (0.1 M KNO_3)(blue line) and for 1.5 mM $[Ru(bpy)_3]^{2+}$ in 0.1 M KNO_3 (red line) using screen-printed carbon electrodes as substrate. Low background fluorescence was observed suggesting a low influence of the screen-printed electrodes and spectroelectrochemical cell materials.

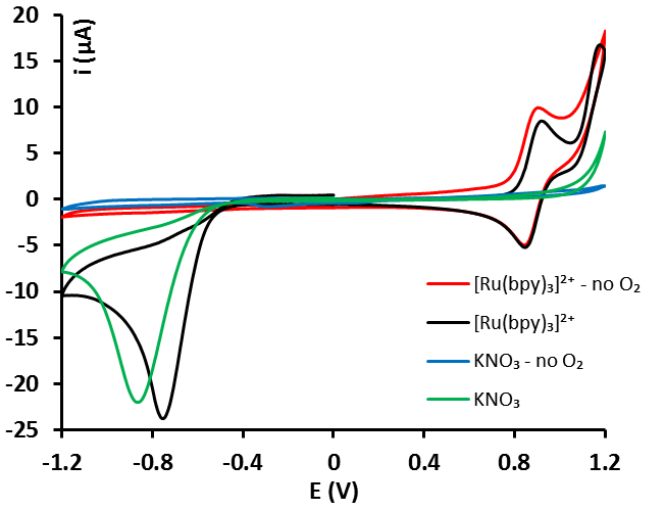

Figure S3. Cyclic voltammograms of 0.1 M KNO_3 and 1.5 mM $[Ru(bpy)_3]^{2+}$ in 0.1 M KNO_3 in normal and deareated solutions. Deareated solutions show the loss of the intense cathodic process at a potential near -0.80 V, which is attributed to the removal of O_2 from the solution.

VIDEOS

Video S1. Dynamic evolution of the normalized fluorescence and the derivative of the fluorescence at 610 nm for 1.5 mM of $[Ru(bpy)_3]^{2+}$ in 0.1 M KNO_3 during the cyclic voltammetry experiment. Initial potential: 0 V, 1st vortex potential: +1.2 V, 2nd vortex potential: -1.2 V, scan rate: 10 mV/s.

Video S2. Dynamic evolution of the normalized fluorescence and the derivative of the fluorescence at 610 nm for 1.5 mM of $[Ru(bpy)_3]^{2+}$ in 0.1 M KNO_3 during the multi-pulsed amperometric experiment (by applying consecutive pulses of +1.2 V and +0.3 V for 60 s each).

Video S3. Results of the digital simulation of the cyclic voltammetry of $[Ru(bpy)_3]^{2+/3+}$ compared to the experimental results obtained at different scan rates (10, 50, 100 and 250 mV/s). Video also shows the evolution of the profile concentration with the distance to the electrode of $[Ru(bpy)_3]^{2+}$ (red line) and $[Ru(bpy)_3]^{3+}$ (blue line).

REFERENCES

(1) Brown, J. H. *J. Chem. Educ.* **2015**, *92* (9), 1490–1496.

(2) Martín-Yerga, D.; Costa Rama, E.; Costa García, A. *J. Chem. Educ.* **2016**, *93* (7), 1270–1276.